

# Thermal collapse of spin-polarization in half-metallic ferromagnets

M. Ležaić,\* Ph. Mavropoulos,† J. Enkovaara, G. Bihlmayer, and S. Blügel  
*Institut für Festkörperforschung, Forschungszentrum Jülich, D-52425 Jülich, Germany*

The temperature dependence of the magnetization and spin-polarization at the Fermi level is investigated for half-metallic ferromagnets. We reveal a new mechanism, where the hybridization of states forming the half-metallic gap depends on thermal spin fluctuations and the polarization can drop abruptly at temperatures much lower than the Curie point. We verify this for NiMnSb by *ab initio* calculations. The thermal properties are studied by mapping *ab initio* results to an extended Heisenberg model which includes longitudinal fluctuations and is solved by a Monte Carlo method.

PACS numbers: 75.50.Cc, 71.20.Be, 75.30.Et, 71.20.Lp

Half-metallic ferromagnets (HMFs) are ferromagnetic metallic compounds showing, in the ideal case and at zero temperature, a spin polarization of  $P = 100\%$  at the Fermi level  $E_F$ . This means that the spin-resolved density of states (DOS) shows a metallic character only for one spin direction (usually majority-spin), with energy bands crossing  $E_F$ ; contrary to this, the other spin direction (minority-spin) behaves like an insulator with  $E_F$  inside a band gap. This exotic behavior has inspired research not only in the field of basic science, but also for applications in spintronics, since the extreme spin polarization suggests that HMFs are ideal for inducing and manipulating the transport of spin-polarized electrons.

Since HMFs were originally introduced in 1983 [1], their properties have been explored extensively. Theoretical studies have focused mainly on their ground-state properties: the magnetic moments and the origin of the gap [2]. The stability of the gap was studied with respect to spin-orbit coupling [3], to surface and interface states [4], to the presence of defects [5] and to the appearance of non-quasiparticle states [6]. In parallel, the extreme spin polarization has been verified experimentally in a few compounds [7]. However, it is clear that the ideal half-metallic property ( $P = 100\%$ ) cannot be present at elevated temperatures. Fluctuations of magnetic moments will mix the two spin channels, and at latest at the Curie point,  $T_C$ , the spin polarization will vanish together with the magnetization. Thus, for application purposes one seeks HMFs with  $T_C$  significantly higher than room temperature, reasonably assuming that the temperature dependence of the spin polarization,  $P(T)$ , approximately follows the magnetization, i.e.,  $P(T) \propto M(T)$  [8]. But the theoretical study of  $P(T)$  is far from trivial. Materials specific, first-principles calculations based on density-functional theory (DFT), which capture the physics of hybridizations and bonding essential to the half-metallic property [2], are designed in principle for the ground state and not for excited state properties. Nevertheless, adiabatic spin dynamics can be approximated within DFT, with successful applications in the prediction of  $T_C$  [9, 10], lately also for Heusler alloys [11, 12, 13].

In many cases, HMFs have more than one magnetic atom per unit cell. For example, NiMnSb, a half-Heusler compound and prototypical example of all HMF has two magnetic atoms: Mn and Ni. It is the  $d$ - $d$  hybridization between the Mn and Ni minority states that opens the half-metallic gap [2], at least at  $T = 0$ . At higher temperatures, directional fluctuations of local moments reduce the magnetization. In one-component systems it is well-known that the magnetic configuration at each instant shows some degree of short-range order: small regions present almost collinear magnetic moments, with a local spin quantization axis  $\hat{e}_{\text{loc}}$  not necessarily parallel to the average moment (the global axis  $\hat{e}_{\text{glob}}$ ), while the low-energy, long-wavelength fluctuations are more significant for the decrease of the magnetization. This behavior continues up to and even above  $T_C$ . However, rather little is known for multi-component systems, when the sublattices are coupled with different strength so that they can lose the magnetic order at different temperatures.

Motivated by these considerations, we follow two approaches to the excited states, both based on DFT (one in connection to an extended Heisenberg model, and one within mean-field theory), in order to elucidate the problem of magnetization and spin polarization at  $T > 0$ . Our focus is on NiMnSb. We conclude that the hypothesis  $P(T) \propto M(T)$  is not valid. Instead,  $P(T)$  can fall off much faster than  $M(T)$ . Furthermore, for NiMnSb we find that the Ni moment disorders already at very low temperatures, resulting in a susceptibility peak at 50 K.

We expect that the decrease of  $P$  in the presence of non-collinear fluctuations arises due to three mechanisms: (1) Firstly, we have a globally non-collinear effect: the local axis  $\hat{e}_{\text{loc}}$  of a region with short-range order is in general not parallel  $\hat{e}_{\text{glob}}$ . Thus, there is always a projection of locally spin-up states to the globally spin-down direction in the gap region. (2) Secondly, a locally non-collinear effect: the short-range order is not perfect, since the spin axis of each atom varies with respect to that of its neighbors. This effect can be more significant in multi-component systems. It is most important if, e.g., a spin-up localized  $d$  resonance determining the local frame is at  $E_F$ . The result of this effect is that, even in a lo-

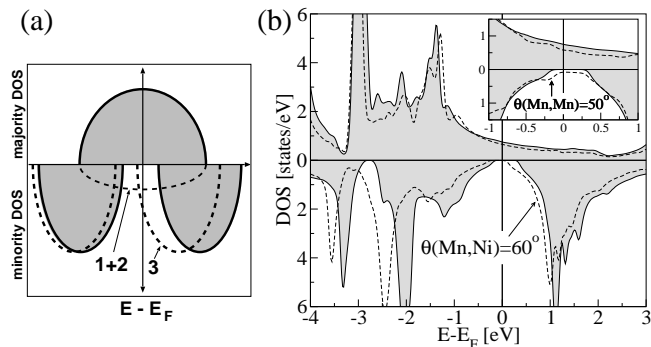


FIG. 1: (a): Modification of spin-down DOS around  $E_F$  reducing the spin polarization due to mechanisms (1)–(3) as discussed in text. (b): DOS of NiMnSb in the ground state (full curve) and in the state when the Ni moment has been constrained to an angle of  $60^\circ$  with respect to the Mn moment (dashed curve). Inset: Dashed curve: the state when Mn moments of neighboring layers along [001] direction form an angle of  $50^\circ$  with respect to each other, while the Ni moments are allowed to relax. DOS are projected to the global frame.

cal spin frame of reference, spin-up wavefunctions of each atom are partly projected into the spin-down states of its neighbors within the gap, so that  $P$  is diminished. In the presence of only the first effect,  $P(T)$  is expected to follow the average magnetization  $M(T)$ ; the second effect arises in addition to the first, and  $P(T)$  is even further reduced. (3) Importantly, there is a hybridization effect (change in hybridization strength), which has been overlooked so-far, leading to a closure of the gap by shifting the conduction and valence band edges. In Fig. 1a we show schematically how the three mechanisms affect the minority-spin DOS. Naturally, changes in the majority DOS also occur and charge neutrality is conserved.

We turn now to the specific system, namely NiMnSb. We find by first-principles calculations that, in the ground state, the Mn local magnetic moment is large ( $M_{\text{Mn}} = 3.7 \mu_B$ ), while the Ni local moment is much smaller ( $M_{\text{Ni}} = 0.26 \mu_B$ ) and originates mainly from the hybridization of the  $d$  orbitals of Mn with the ones of Ni (the same mechanism which opens the half-metallic gap [2]). In particular, the  $d$ - $d$  hybridization causes some transfer of weight from Mn to Ni in the unoccupied states and vice-versa in the occupied ones. Thus, the Ni moment is formed, while the Mn moment is reduced. Consequently, the Ni moment does not really arise from strong intra-atomic exchange interactions (Hund’s rule), and its formation lies at a much lower energy scale than that of the Mn moment. We verify this conclusion by performing constrained DFT [14] calculations: when the magnetic moment of Mn is constrained by a magnetic field to form an angle to its Mn neighbors, it changes very little, even in an artificial antiferromagnetic configuration. Contrary to this, the Ni moment vanishes already when it is constrained at an angle of  $90^\circ$  with respect to the

Mn moment, or when the Mn atoms are placed in an artificial antiferromagnetic order.

We approach the finite-temperature properties starting with a standard recipe: the adiabatic approximation for the calculation of magnon spectra [15]. We employ the full-potential linearized augmented plane-wave method (FLAPW) as implemented in the FLEUR code [16] within the generalized gradient approximation [17] to DFT. Total-energy calculations of frozen magnons, performed at the equilibrium lattice constant of  $5.9 \text{ \AA}$ , on a dense mesh of 2745 wavevectors  $\vec{q}$  and 4096  $\vec{k}$ -points, provide the magnon dispersion relations  $E(\vec{q})$ . A subsequent Fourier transform yields the real-space exchange constants  $J_{ij}$  between sites  $i$  and  $j$  ( $\in \{\text{Ni, Mn}\}$ ) [9], mapping the system to a classical Heisenberg model. Thermodynamic quantities such as the magnetization curve  $M(T)$ , susceptibility  $\chi(T)$ , and Curie point  $T_C$  can be found within this model by a Monte Carlo method [18]. In multi-component systems we also consider the sublattice susceptibility  $\chi_n$  and magnetization  $M_n$  ( $n$  is a sublattice index). A peak of  $\chi_n(T)$  signals the release of the corresponding degrees of freedom, i.e., the sublattice magnetization is randomized to a great extent; the total susceptibility  $\chi(T)$  presents a peak at  $T_C$ .

While the Mn moment can be treated within the Heisenberg model as having a fixed absolute value and fluctuating only in its direction, for the weak Ni moment the longitudinal fluctuations are energetically as relevant as the transversal ones. These considerations require an extension of the traditional Heisenberg model allowing fluctuations of the magnitude of  $M_{\text{Ni}}$ . This is possible, since the energy needed for constraining the Ni moment can be calculated within DFT and fitted well by a fourth-order function. Within this approximation, at each Ni site  $i$  the neighboring atoms, placed at sites  $j$ , act as an exchange field  $\vec{B}_i = \sum_j J_{ij} \vec{M}_j$  polarizing the Ni atom. Thus, the energy expression for the Ni atom at  $i$  includes the magnitude of the *local* moment  $M_i$  and the neighbor-induced polarizing field, and the total Hamiltonian reads

$$H = -\frac{1}{2} \sum_{i,j} J_{ij} \vec{M}_i \cdot \vec{M}_j + \sum_{i \in \{\text{Ni}\}} (a M_i^2 + b M_i^4 - \vec{B}_i \cdot \vec{M}_i). \quad (1)$$

The constants  $a = 18.4 \text{ mRy}/\mu_B^2$  and  $b = 42.6 \text{ mRy}/\mu_B^4$ , which are fitted to the *ab initio* total energy results, are both positive, giving an energy minimum at  $M_i = 0$  if the neighbors have a zero net contribution, i.e., if  $\vec{B}_i = 0$ . The second sum of Eq. (1) has to be applied for all Ni sites  $i$  entering the Monte Carlo calculation, on top of the usual first part, which is just the Heisenberg expression. Note that, although the Ni moment is small and resulting from hybridization, a remnant of intra-atomic exchange still exists in Ni, giving an enhanced on-site susceptibility. This assists the local moment formation and is reflected in the values of  $a$  and  $b$ . Thus, the system can be regarded as an alloy of a strongly magnetic subsystem (Mn) with

a paramagnetic subsystem with Stoner-enhanced susceptibility (Ni).

After calculating the exchange parameters  $J_{ij}$  (our results agree with those of Ref. [11]), the Monte Carlo calculation according to Eq. (1) yields the sublattice magnetizations  $M_{\text{Mn}}(T)$  and  $M_{\text{Ni}}(T)$ , and the susceptibilities  $\chi_{\text{Mn}}(T)$  and  $\chi_{\text{Ni}}(T)$ , shown in Fig. 2a. Evidently, the overall thermodynamics are governed by the mighty Mn moment. The phase transition is clearly seen by the peak in the susceptibility  $\chi(T)$ , which grossly coincides with the Mn sublattice susceptibility  $\chi_{\text{Mn}}(T)$ . A value of  $T_C \approx 860$  K is deduced, verified also by the method of cumulant expansion [18], and lies between the value of 940 K calculated in [13] and the experimental value of  $T_C = 730$  K. The surprising feature, however, is the behavior of  $M_{\text{Ni}}(T)$  and  $\chi_{\text{Ni}}(T)$ . Already at low temperatures, around 50 K,  $M_{\text{Ni}}(T)$  shows a rapid drop and  $\chi_{\text{Ni}}(T)$  a corresponding narrow peak. If we exclude the longitudinal fluctuations and work within the traditional Heisenberg model, an unpronounced behavior can be seen (broad maximum in  $\chi_{\text{Ni}}^{\text{transv.}}(T)$  at around  $T = 300$  K in Fig. 2a). These results show that the Ni sublattice magnetic order is lost to its great extent. This behavior is traced back to the comparatively weak exchange constants  $J_{ij}$  of the Ni moments to the neighboring atoms, as we found by the *ab initio* calculations.

It is well-known that the classical Heisenberg model cannot capture the very low-energy spectrum of the quantum Heisenberg model, therefore the low- $T$  behavior of  $M$  is usually not well reproduced. However, since the longitudinal fluctuations (essential to our model) on the Ni sublattice allow for a high rate of energy absorption around the crossover temperature (50 K), the classical treatment of the Ni sublattice is applicable already at such low  $T$ . We believe the peak of  $\chi_{\text{Ni}}$  and the drop of  $M_{\text{Ni}}$  at low  $T$  to be connected to the so-far unexplained experimental findings of an anomaly in the temperature dependence of the magnetization and the resistivity at approximately 80 K [19]. Assuming that the magnetic moments on the Ni sublattice are disordered, the system can absorb energy at a higher rate and this would lead to a higher dissipation and subsequent increase in resistance.

The loss of short-range order in the Ni sublattice at such low temperatures suggests, at first sight, that half-metallicity is easily lost, due to the mechanism (2) of local non-collinearity. However, this is not completely correct. Since the gap originates from the  $d$ - $d$  hybridization between Ni and Mn spin-down states, and since the Ni  $d$  states are below  $E_F$  for both spin directions, a rotation of the Ni moment causes a hybridization of the Mn  $d$  spin-down states partly with the Ni spin-up states and partly with the Ni spin-down states. Consequently, the  $d$ - $d$  hybridization remains, but the gap width is reduced. The relevant DOS is shown in Fig. 1b, for the case of the Mn moments remaining in a ferromagnetic

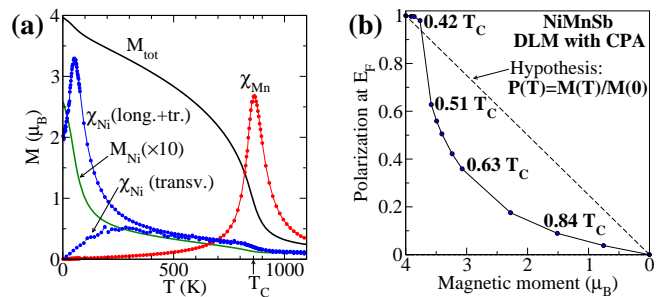


FIG. 2: (color online) (a): Monte Carlo results for the  $T$ -dependent magnetic properties. The Ni sublattice moment  $M_{\text{Ni}}$  (magnified by a factor 10) drops fast at 50 K, fluctuating transversely and longitudinally; a susceptibility peak ( $\chi_{\text{Ni}}(\text{long.}+\text{tr.})$ ) is evident. If only transverse fluctuations are allowed,  $\chi_{\text{Ni}}(\text{transv.})$  has a less pronounced maximum. (b): Polarization at  $E_F$  as function of total spin moment for the DLM states for  $\text{NiMn}_{1-x}^{\uparrow}\text{Mn}_x^{\downarrow}\text{Sb}$  calculated with the CPA. The degree  $x$  of disorder increases from left ( $x = 0\%$ ) to right ( $x = 50\%$ ), simulating the increase of  $T$  from 0 to  $T_C$ .

configuration, while the Ni moments are constrained to a  $60^\circ$  angle relative to Mn (and as a result their magnitude is reduced to  $0.16 \mu_B$ ). The reduction of the gap width follows from a reduction of the hybridization strength: as the Ni moment is reduced, its spin-down states move lower in energy and hybridize less with the Mn spin-down states. Thus, the spin-down “conduction band” ultimately reaches  $E_F$  and half-metallicity is lost. This is the signature of the hybridization mechanism (3), and comes on top of the non-collinear behavior of the Mn atoms (mechanisms (1) and (2)). The latter should be weak at such low  $T$ , since the average Mn moment should still be high, dictated by Bloch’s  $T^{3/2}$  law. At higher temperatures the locally non-collinear mechanism (2) should appear for the Mn moments. In the inset of Fig. 1b we show the state when Mn moments of neighboring layers form an angle of  $50^\circ$  with respect to each other. Although mechanism (2) produces a mild effect of a finite spin-down DOS at  $E_F$ , a protrusion appears just 0.2 eV under  $E_F$ . This is once more related to mechanism (3), triggered by the non-collinear configuration, and can cause a collapse of  $P$  if the protrusion reaches  $E_F$ .

The results so-far do not contain a quantitative estimate of the polarization as function of  $T$  or of the order parameter  $M$ . Such an estimate requires knowledge of the response of the electronic structure to the increase of  $T$ . We achieve this by proceeding via mean-field theory, with the disordered local moment (DLM) state [10] representing the system at  $T > 0$  in a mean-field manner. A Mn site can then have a “down” orientation  $\text{Mn}_x^{\downarrow}$  (opposite to the magnetization) with probability  $x$ , or an “up” orientation  $\text{Mn}_{1-x}^{\uparrow}$  (parallel to the magnetization). The ferromagnetic ground state ( $T = 0$ )

corresponds to  $x = 0$ , while the Curie point corresponds to  $x = 0.5$ . The electronic structure of the DLM state for each  $x$  is found within the coherent potential approximation (CPA), utilizing the Korringa-Kohn-Rostoker full-potential Green function method within DFT. This yields the average magnetic moment  $M(x)$  (approximately,  $M(x) = M(0)(1 - 2x)$  so  $x$  is an alternative order parameter), and the polarization  $P(x)$ .

Considering the above, we study the DLM states,  $\text{NiMn}_{1-x}^{\uparrow}\text{Mn}_x^{\downarrow}\text{Sb}$ , with varying concentration  $0 < x < 0.5$ . Within this approach,  $P(T)$  cannot be directly found, if the explicit connection between  $x$  and  $T$  (or  $M(T)$ ) is not known. However, one can check the hypothesis  $P(T) \sim M(T)$  [8]. As shown in Fig. 2b, such a relation does not hold. Instead, from a certain  $M$  on,  $P$  drops much faster than  $M$ . The reason can be traced back to the change in hybridization as  $x$  (or  $T$ ) increases: each Ni atom has on average  $4(1 - x)$   $\text{Mn}^{\uparrow}$  neighbors and  $4x$   $\text{Mn}^{\downarrow}$  neighbors. The occupied  $d$  states of the latter hybridize with the occupied spin-down states of Ni, push them higher in energy and diminish the gap;  $E_F$  reaches finally the valence band and  $P$  collapses. Furthermore, an approximation of  $M(T)$  consistent with mean-field theory can be found by the use of the Brillouin function  $B_j$ . Doing this for  $j = 5/2$ , we assigned the temperature values shown in Fig. 2b. Under this assumption we see that, up to  $T = 0.42 T_C$  (this is about room temperature),  $P(E_F)$  remains close to 100%, but then it drops fast, e.g.,  $P \approx 35\%$  at  $T = 0.67 T_C$ . The globally non-collinear mechanism (1), not captured by the CPA, should be present on top of this behavior. Therefore, the initial plateau of  $P$  (up to  $0.42 T_C$ ) should be corrected towards a linear drop as  $P(T) = M(T)/M(0)$ .

In summary, we have investigated the behavior of half-metallic ferromagnets at elevated temperatures, with emphasis on the properties of the gap and the spin polarization at  $E_F$ . We introduced an extended Heisenberg model treating transversal as well as longitudinal magnetic fluctuations, to cover a little investigated situation: multicomponent magnets which include subsystems of large moments coexisting with paramagnetic subsystems exhibiting a Stoner-enhanced susceptibility. The parameters entering the model were determined from first principles. We also estimated the polarization at  $E_F$  within a CPA averaging. As prototypical system we have chosen the half-Heusler compound  $\text{NiMnSb}$ . Our conclusions are the following: (i) In  $\text{NiMnSb}$ , the Ni sublattice is weaker coupled than the Mn one; longitudinal fluctuations of the Ni moment are energetically as important as transversal fluctuations. This leads to an early crossover behavior of the magnetization at  $T \approx 0.06 T_C$  where the average Ni moment is lost, explaining previous experiments. (ii) The hybridization creating the gap is still present but the fluctuations change its strength. At this stage the gap-width is reduced. (iii) At higher  $T$ , fluctuations of the Mn moments introduce a low DOS into

the gap leading to a mild reduction of  $P$ , and, after a point, the hybridization changes so much that  $E_F$  crosses the band edges. This is when the polarization collapses (around  $0.42 T_C$  within mean-field theory). The behavior of  $P$  shown here seems rather general for half- and full-Heusler alloys exhibiting half-metallic ferromagnetism as we found by additional calculations. E.g., for  $\text{Co}_2\text{MnSi}$ , the polarization was close to 100% till  $0.27 T_C$ , then it dropped fast, changed sign at  $0.63 T_C$  and went back to zero at  $T_C$ . The decisive factor for the thermal collapse of polarization is the change in hybridizations due to the moment fluctuations. This work calls for experimental efforts to measure the sublattice magnetization and the spin polarization at  $E_F$  as function of  $T$  for half-metals.

We are grateful to P. H. Dederichs for enlightening discussions, and to H. Ebert and V. Popescu for providing us with their CPA algorithm [20].

---

\* Electronic address: M.Lezaic@fz-juelich.de

† Electronic address: Ph.Mavropoulos@fz-juelich.de

- [1] R. A. de Groot, F. M. Mueller, P. G. van Engen, and K. H. J. Buschow, Phys. Rev. Lett. **50**, 2024 (1983).
- [2] I. Galanakis, P. H. Dederichs, and N. Papanikolaou, Phys. Rev. B **66**, 134428 (2002); *ibid.* **66**, 174429 (2002).
- [3] Ph. Mavropoulos, K. Sato, R. Zeller, P. H. Dederichs, V. Popescu, and H. Ebert, Phys. Rev. B **69**, 054424 (2004).
- [4] S. J. Jenkins and D. A. King, Surf. Sci. **494**, L793 (2001); I. Galanakis, M. Lezaic, G. Bihlmayer, and S. Blügel, Phys. Rev. B **71**, 214431 (2005).
- [5] S. Picozzi, A. Continenza, and A. J. Freeman Phys. Rev. B **69**, 094423 (2004).
- [6] L. Chioncel, M. I. Katsnelson, R. A. de Groot, and A. I. Lichtenstein, Phys. Rev. B **68**, 144425 (2003).
- [7] K.E.H.M. Hanssen, P.E. Mijnders, L.P.L.M. Rabou, and K.H.J. Buschow, Phys. Rev. B **42**, 1533 (1990); R.J. Soulen, Jr., J.M. Byers, M.S. Osofsky, B. Nadgorny, T. Ambrose, S.F. Cheng, P.R. Broussard, C.T. Tanaka, J. Nowak, J.S. Moodera, A. Barry, and J.M.D. Coey, Science **282**, 85 (1998); M. Bowen, A. Barthelemy, M. Bibes, E. Jacquet, J.-P. Contour, A. Fert, F. Ciccacci, L. Duo, and R. Bertacco, Phys. Rev. Lett. **95**, 137203 (2005).
- [8] A suggestion that, in a crude approximation,  $P(T) \approx M(T)/M(0)$  (actually an equivalent equation), is given by R. Skomski and P.A. Dowben, Europhys. Lett. **58**, 544 (2002).
- [9] S. V. Halilov, H. Eschrig, A. Y. Perlov, and P. M. Oppeneer Phys. Rev. B **58**, 293 (1998).
- [10] B.L. Gyorffy, A.J. Pindor, J. Staunton, G.M. Stocks, and H. Winter, J. Phys. F: Met. Phys. **15** 1337 (1985).
- [11] E. Sasioglu, L.M. Sandratskii, P. Bruno, and I. Galanakis, Phys. Rev. B **72**, 184415 (2005).
- [12] J. Kübler, Phys. Rev. B **67**, 220403 (2003); Y. Kurtulus, R. Dronskowski, G.D. Samolyuk, and V.P. Antropov, Phys. Rev. B **71**, 014425 (2005).
- [13] J. Rusz, L. Bergqvist, J. Kudrnovský, and I. Turek (unpublished).
- [14] Ph. Kurz, F. Förster, L. Nordström, G. Bihlmayer, and S. Blügel, Phys. Rev. B **69**, 024415 (2004).

- [15] Based on the timescale of magnons being much slower than electron hopping, whence the electron gas has time to relax under the constraint of the presence of a magnon.
- [16] <http://www.flapw.de>
- [17] J. P. Perdew, K. Burke, and M. Ernzerhof, Phys. Rev. Lett. **77**, 3865 (1996).
- [18] D.P. Landau and K. Binder, *A Guide to Monte Carlo Simulations in Statistical Physics*, Cambridge University Press (2000).
- [19] C. Hordequin, J. Pierre and R. Currat, J. Magn. Magn. Mater. **162**, 75 (1996).
- [20] <http://olymp.cup.uni-muenchen.de/ak/ebert/SPRKKR>